Linear collision of a classical harmonic oscillator with a mass point in the high-frequency region

Max Teubner*
Max-Planck-Institut für Biophysikalische Chemie, Postfach 2841, 37077 Göttingen, Germany
(Received 31 January 2005; published 5 October 2005)

Collinear collisions, with exponential repulsive potential, between a mass point and a harmonic oscillator are studied in the limit of high frequency. Multiple encounters during single collisions and an arbitrary value of the mass parameter m are permitted. Methods are analytical and numerical. The main results are the following: For an initially resting oscillator the energy E after the collision decays exponentially with frequency. The limiting decay constant for high frequency is independent of m and identical to the golden rule prediction $2\pi/\lambda$ where λ^{-1} is a dimensionless frequency. In the high-frequency domain the energy of the oscillator has the form $E=2\pi^2\phi(m)^2\exp\{-2\pi/\lambda\}$ where $\phi(m)=2m-\frac{2}{3}(1+\ln 4)m^2+\cdots$. The first term is the golden rule result, and the second term is new. A series of polynomials ϕ_n is constructed that converges to $\phi(m)$. It is suggested that $\phi(m)$ is an entire function of the complex variable m which has the form of an infinite product $\phi(m)=2m\Pi(1-m/m_n)$ where the m_n are the positive roots of $\phi(m)$. The first 15 roots have been determined numerically which suggests an asymptotic behavior $\sqrt{m_n}\sim an+b$. Agreement with the numerical data is excellent.

DOI: 10.1103/PhysRevA.72.042703 PACS number(s): 34.50.Ez

I. INTRODUCTION

Vibrational-translational energy transfer is of fundamental importance in chemical reactions. For reviews see, e.g., [1–4].

The problem can be studied classically or quantum mechanically. Although experimentally the quantum version is the more important one, there is some merit in studying the classical version. Molecular dynamics (MD) simulations generally simulate classical systems, and a deeper understanding of the quantum problem almost always demands a thorough understanding of the classical system.

Previous papers on this problem were mainly concerned with numerical studies [5–9] or MD simulations [10,11]. In contrast to this, the present paper applies analytical and numerical methods specifically to the asymptotic high-frequency region. This region is not only of particular interest from the experimental point of view, but offers the hope that some simple picture might emerge which could hopefully guide the study of the much more difficult quantum analog.

A. Model

One of the the simplest nontrivial models of vibrational-translational energy transfer is the collinear collision between a harmonic oscillator and a mass point interacting through a repulsive exponential potential. Apart from the hard-point case it is also the only one that has been studied in the quantum domain with some detail [12].

Figure 1 displays two mathematically equivalent versions of the model.

In the upper part the mass point collides with a diatomic molecule whereas in the lower part the mass point collides with an oscillator attached to some point in space like a surface. These models are equivalent after the motion of the center of mass has been separated, provided the collider interacts only with the nearest oscillator atom [7].

B. Exponential interaction

There are a number of reasons to study an interaction having the form of an exponential potential which historically has been the favorite potential for most authors.

(i) The golden rule approximation (which corresponds to the limit of small collider mass m_a) is exactly solvable for the exponential potential in both the classical and quantum cases.

(ii) After transforming to dimensionless variables and parameters, the exponential potential introduces no extra dimensionless parameter [it shares this feature with homogeneous potentials of the form $V(r)=V_0r^{-n}$].

(iii) In the quantum problem the exponential potential permits a particularly simple form in terms of amplitude density functions [12]

Despite these special features, the high-frequency behavior of the exponential potential may be typical for all potentials which have an essential singularity somewhere in the complex r plane. At least this is true in the golden rule approximation classically [13] as well as quantum mechanically [14].

1. Basic equations

In the following we assume that the oscillator-collider potential is an exponential:

$$V(r) = V_0e^{-(x_a-x_b)/L}. \tag{1}$$

We denote the oscillator frequency by ω.

Separating off the motion of the center of mass and transforming to dimensionless lengths and times we obtain the equations of motion in the form (see, for example, Refs. [12,7])

*Electronic address: mteubne@gwdg.de

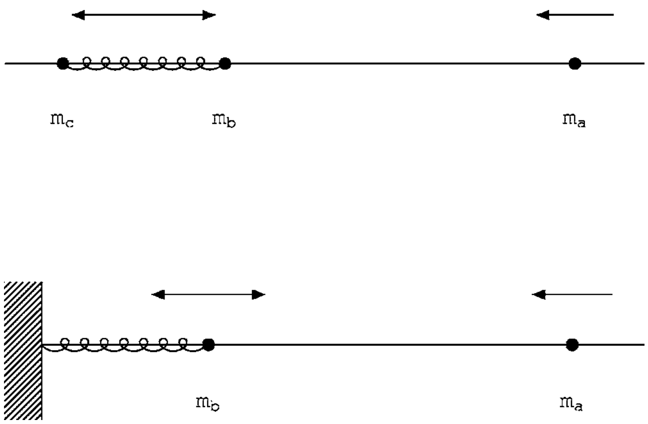

FIG. 1. Upper part: collisions of a mass point with a mobile diatomic oscillator. Lower part: the mass point collides with an oscillator attached to a surface.

$$x'' + x = -e^{x-y}, \tag{2}$$

$$my'' = e^{x-y}, \tag{3}$$

where

$$m = \frac{m_a m_c}{m_b(m_a + m_b + m_c)} \tag{4}$$

is the dimensionless mass parameter.

This refers to collisions of the mobile diatomic molecule in the upper part of Fig. 1. The case of the fixed oscillator (lower part of Fig. 1) leads to the same equations but with

$$m = \frac{m_a}{m_b}. \tag{5}$$

The equations of motion must be supplemented by initial conditions. In the following we will always assume that the oscillator is at rest long before the collision. The system is completely determined by m and the initial value

$$y'(-\infty) = -\lambda, \quad \lambda > 0. \tag{6}$$

The initial velocity v_a of the collider in the center-of-mass frame is related to λ by $v_a = -\lambda\omega L$. The limit $\lambda \to 0$ can alternatively be described as $v_a \to 0$, $\omega \to \infty$, or $L \to \infty$, holding the other two variables constant. By "high-frequency limit" we mean in the following: $\lambda \to 0$, and note that the limit of slow approach $v_a \to 0$ describes the same physics.

We are interested in the final energy of the oscillator,

$$E = \frac{1}{2}(x^2 + x'^2), \tag{7}$$

long after the collision as a function of m for $\lambda \to 0$.

2. Golden rule

For small collider mass the mass parameter m is also small. The oscillator may be regarded as undisturbed and fixed at the origin. Equation (3) then becomes

$$my'' = e^{-y}, \tag{8}$$

with solution

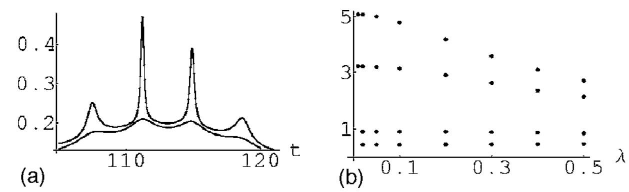

FIG. 2. (a) Plots of $\mathrm{Im}[y'(t+is)]$ versus t for $m=50$ and $\lambda=0.3$. Lower curve: $s=6.8$. Upper curve: $s=7.7$. (b) Values of $\pi/\lambda - t^*$ versus λ where t^* is the imaginary part of the singularity closest to the real axis. From bottom to top, $m=5,10,50,100$.

$$y(t) = 2\ln\left(\frac{2\cosh(\lambda t/2)}{\lambda\sqrt{2m}}\right). \tag{9}$$

This leads to [15]

$$\int_{-\infty}^{\infty} e^{-y(t)} \cos t dt = \frac{2\pi m}{\sinh(\pi/\lambda)} \tag{10}$$

and, using Eq. (12) below, yields the golden rule result

$$E = \frac{2\pi^2}{\sinh^2 \frac{\pi}{\lambda}} m^2. \tag{11}$$

II. COMPLEX SINGULARITIES AND THE DECAY CONSTANT

It is well known that the final energy of an initially resting oscillator of mass μ can also be written in the form [5]

$$E = \frac{1}{2\mu}\left|\int_{-\infty}^{\infty} e^{i\omega t} f(t) dt\right|^2, \tag{12}$$

where $f(t)$ is the force acting on the oscillator. This is true even if the force depends on the state of the oscillator. In terms of our dimensionless $x(t)$ and $y(t)$ this becomes

$$E = \frac{1}{2}\left|\int_{-\infty}^{\infty} e^{it} e^{x(t)-y(t)} dt\right|^2. \tag{13}$$

Consider the frequency dependence of Eq. (12). It is well known that the asymptotic behavior at high frequency is governed by the location of the singularities of $f(t)$ in the complex t plane. If t^* is the imaginary part of the closest singularity of $f(t)$ to the real axis,

$$E \sim e^{-2\omega t^*} \tag{14}$$

for high frequency up to algebraic powers in ω.

Such an exponential factor is of course also present in Eq. (13), although this is not apparent since ω has been rendered invisible by scaling.

In order to determine the "decay constant" $2t^*$ we need the dominant complex singularity of $x(t) - y(t)$. From the equations of motion it is apparent that the singularities of $x(t)$ and $y(t)$ coincide. Numerically the singularities are readily identified in the derivatives.

Figure 2(a) shows typical plots of $\mathrm{Im}[y'(t+is)]$ versus t

(i.e., parallel to the real axis) for $m=50$ and $\lambda=0.3$. The lower curve corresponds to $s=6.8$ and the upper to $s=7.7$. Each peak corresponds to a "collision" and develops into a singularity if the imaginary part is increased further. The second peak corresponds to the dominant singularity which appears at $s=t^*=7.8397$.

For larger m the number of relevant collisions (singularities with almost identical imaginary parts) increases.

Figure 2(b) shows data for $\pi/\lambda-t^*$ versus λ for various m. The points seem to tend to definite limits for $\lambda\to 0$. For small λ the dominant singularity behaves as

$$t^*=\frac{\pi}{\lambda}+c(m) \tag{15}$$

for some $c(m)$ that is independent of λ.

This is a remarkably simple result. The frequency dependence of t^* appears to be independent of m and equal to the golden rule prediction (for similar results on related systems see [16,9,17] and references therein).

Another interesting feature of the singularities is the following. For certain isolated values $m=m_n$ [the zeros of $\phi(m)$; see Fig. 4] the oscillator receives no net energy and remains at rest after the collision. At these zeros a dominant and a subdominant singularity switch roles so that precisely at m_n there are two different singularities with identical imaginary parts.

Equation (15) indicates that in the limit $\lambda\to 0$ the integral in Eq. (13) can be written in the form

$$2\pi\phi(m)e^{-\pi/\lambda} \tag{16}$$

for some function $\phi(m)$ (the factor 2π has been introduced for later simplification). The oscillator energy long after the collision then is given by

$$E=2\pi^2\phi(m)^2e^{-2\pi/\lambda}. \tag{17}$$

For small m we may employ the golden rule result, Eq. (11), which indicates

$$\phi(m)=2m+\cdots\ . \tag{18}$$

III. EXPANSION IN λ

Since we are interested in the limit $\lambda\to 0$, is seems sensible to somehow expand the equations of motions in λ. This can indeed be done after due care has been taken of the presence of two time scales in the problem.

A. Two time scales

For small λ the problem contains two time scales. One time scale is the period on the oscillator, and the other is the time scale of the motion of the collider λ. This can be seen already in the solution Eq. (9) entering the golden rule. Here the oscillatory part is neglected, but it should be present in a more detailed theory. The two time scales (a rapid oscillation and a slow overall motion of collider and oscillator) can also be clearly seen in numerical simulations for small λ.

Since the golden rule follows from the slow-motion part alone, it seems sensible to ask if it can be improved by taking further terms of the slow motion into account while neglecting the rapid oscillations.

In fact we will argue below that the slow part alone is sufficient to determine the asymptotic energy transfer exactly in the limit of $\lambda\to 0$.

For the slow part we make the ansatz

$$x(t)=u(\lambda t), \tag{19}$$

$$y(t)=2\ln\left(\frac{2\cosh(\lambda t/2)}{\lambda\sqrt{2m}}\right)+v(\lambda t) \tag{20}$$

and obtain

$$\lambda^2u''(\tau)+u(\tau)=-\frac{\lambda^2m}{2\cosh^2\tau/2}e^{u-v}, \tag{21}$$

$$\lambda^2mv''(\tau)=\frac{\lambda^2m}{2\cosh^2\tau/2}(e^{u-v}-1), \tag{22}$$

with

$$\tau=\lambda t. \tag{23}$$

This is a singular perturbation problem since the small parameter λ multiplies the highest derivative.

B. Expanding the slow solution

We now expand u and v into a formal power series in λ,

$$u(\tau)=\sum_{n\geqslant 1}\lambda^{2n}u_n(\tau), \tag{24}$$

$$v(\tau)=\sum_{n\geqslant 1}\lambda^{2n}v_n(\tau), \tag{25}$$

and compare coefficients. Because these series result from a singular perturbation problem, they have an asymptotic significance only and the series can not be expected to converge. Nevertheless, we will argue that they permit an asymptotically exact evaluation of the energy transfer in the limit $\lambda\to 0$.

At first order,

$$u_1=-\frac{m}{2\cosh^2\tau/2}, \tag{26}$$

and v_1 satisfies

$$mv_1''+\frac{m}{2\cosh^2\tau/2}v_1=-\frac{m^2}{4\cosh^4\tau/2}. \tag{27}$$

A special solution is

$$v_1(\tau)=\frac{m}{4\cosh^2(\tau/2)}-\frac{m}{2}. \tag{28}$$

The general solution of the homogeneous equation is

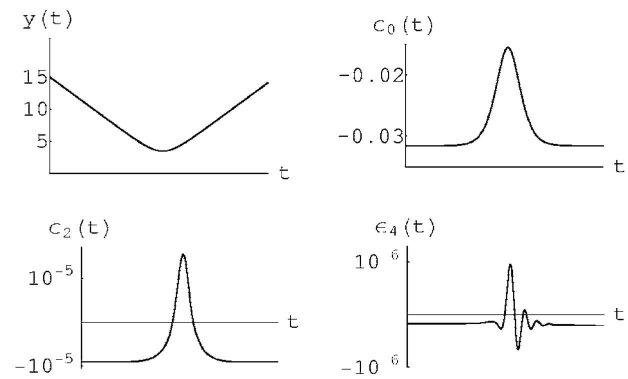

FIG. 3. $y(t)$ and errors ϵ_n in finite series for $m=1$, $\lambda=1/4$.

$$c_1 \tanh\frac{\tau}{2} + c_2\left(\tau\tanh\frac{\tau}{2} - 2\right). \tag{29}$$

The boundary condition for $\tau \to -\infty$ implies $c_2=0$. In the following we consider only solutions even in τ so that v_1 is given by Eq. (28).

In general it follows from the structure of the differential equations that v_n satisfies

$$v_n'' + \frac{m}{2\cosh^2 \tau/2} v_n = f_n(\tau), \tag{30}$$

where f_n is a polynomial of u_k, v_k with smaller indices.

One can show by induction that the u_n and v_n are finite polynomials in $\cosh^{-2}\tau/2$:

$$u_n(\tau) = \sum_{k=1}^{n} \frac{a_{nk}}{\cosh^{2k}\tau/2}, \tag{31}$$

$$v_n(\tau) = \sum_{k=0}^{n} \frac{b_{nk}}{\cosh^{2k}\tau/2}. \tag{32}$$

There exist linear relations among the a_{nk} and b_{nk}. Of particular interest are the relations among the diagonal terms:

$$a_{n+1,n+1} - n\frac{2n+1}{2}(a_{nn} + m b_{nn}) = 0. \tag{33}$$

The a_{nk} and b_{nk} are themselves polynomials in m. They have been determined by a computer algebra system (Mathematica) up to order 15×15. These data confirm the suspicion that the series, Eqs. (24) and (25), do not converge and are only asymptotic.

That the series have only an asymptotic meaning can also be seen from the following argument: If $u(\tau)$ and $v(\tau)$ were well-defined functions (and twice differentiable), they would be true solutions of the basic equations (21) and (22). However, this $u(\tau)$ tends to 0 for $|\tau|\to\infty$; i.e., there would be no energy transfer for any m.

Nevertheless, the finite series do provide good approximations to the true solution. Figure 3 shows the true $y(t)$ (upper left) as well as the errors $\epsilon_0, \epsilon_2, \epsilon_4$ of three approximations for $m=1$, $\lambda=1/4$. The ϵ_n are defined by

$$\epsilon_n(t) = y(t) - 2\ln\left(\frac{2\cosh(\lambda t/2)}{\lambda\sqrt{2m}}\right) - \sum_{k=1}^{n} \lambda^{2k} v_k(\lambda t). \tag{34}$$

C. Final energy

We can now formally express the Fourier transform of the force,

$$F(f) \equiv \int_{-\infty}^{\infty} e^{x(t)-y(t)} e^{it} dt = -\int_{-\infty}^{\infty} \frac{\lambda^2 m}{2\cosh^2 \tau/2} e^{u(\tau)-v(\tau)} \cos t dt, \tag{35}$$

in terms of a_{nk} or b_{nk}.

We replace the integrand by Eq. (22) and obtain

$$F(f) = \int_{-\infty}^{\infty} \left(m\frac{d^2}{dt^2} v(\lambda t) + \frac{\lambda^2 m}{2\cosh^2 \frac{\lambda t}{2}} \right) \cos t dt \tag{36}$$

$$= \frac{2\pi m}{\sinh\frac{\pi}{\lambda}} - \int_{-\infty}^{\infty} m v(\lambda t)\cos t dt, \tag{37}$$

where Eq. (10) has been used. We insert Eqs. (25) and (32), use [15]

$$\int_{-\infty}^{\infty} \frac{\cos t}{\cosh^{2k}(\lambda t/2)} dt = \lambda^{-2k} \frac{2^{2k}}{(2k-1)!} \prod_{p=0}^{k-1} (1+p^2\lambda^2) \frac{\pi}{\sinh\frac{\pi}{\lambda}}, \tag{38}$$

and obtain the formal expansion of $F(f)$ in powers of λ:

$$F(f) = \left(2m - m\sum_{n\geqslant 1}\sum_{n\geqslant k} b_{nk}\lambda^{2(n-k)} \frac{2^{2k}}{(2k-1)!} \times \prod_{p=0}^{k-1}(1+p^2\lambda^2) \right) \frac{\pi}{\sinh\frac{\pi}{\lambda}}. \tag{39}$$

This looks encouraging since it suggests a decay of $F(f) \sim \exp\{-\pi/\lambda\}$, which was the time constant found numerically to govern the decay of $F(f)$. Unfortunately, the numerical data for b_{nk} suggests that the right side diverges for any $\lambda > 0$. The reason is not so much that b_{nk} increase with n (which they do), but the product, which produces a factor $\sim n!^2$ for large n.

However, let us take the limit $\lambda \to 0$ on the right side. We obtain

$$F(f) = \lim_{n\to\infty} \phi_n(m) \frac{\pi}{\sinh\frac{\pi}{\lambda}}, \tag{40}$$

with

$$\phi_n(m) = 2m - m\sum_{k=1}^{n-1} b_{kk}\frac{2^{2k}}{(2k-1)!} = -\frac{2^{2n}}{(2n-1)!}a_{nn}, \quad (41)$$

where the last equality follows from Eq. (33). The ϕ_n are polynomials of order n in m.

Before I present evidence that the right side converges and furnishes indeed the correct limit for $\lambda \to 0$, let us consider a simpler procedure to determine the a_{nn} and b_{nn}. This will also permit us to understand better the structure of these coefficients and to extend the numerical data to higher indices.

IV. APPROXIMATING POLYNOMIALS $\phi_n(m)$

A. Generating functions $A(x)$ and $B(x)$

The previous section described a procedure to determine the coefficients a_{nk}, b_{nk}. We need, however, only the diagonal term a_{nn} or b_{nn}.

A closer look at the system of equations which determine a_{nk}, b_{nk} reveals that the diagonal terms can be determined independently from the rest. It would be desirable to have a method to extract the diagonal terms only without having to deal with the off-diagonal ones.

To this end we write $u(\tau)$ [and similarly $v(\tau)$] in the form

$$u(\tau) = \sum_{k\geq 1} x^{2k}a_{kk} + \lambda\sum_{k\geq 1} x^{2k}a_{k+1,k} + \lambda^2\sum_{k\geq 1} x^{2k}a_{k+2,k} + \cdots, \quad (42)$$

with

$$x = \frac{\lambda}{\cosh\frac{\tau}{2}}. \quad (43)$$

Taking formally $\lambda \to 0$ at fixed x converts $u(\tau)$ into the generating function of the diagonal elements.

We therefore insert $u(\tau)=A(x)$ and $v(\tau)=B(x)$ into Eqs. (21) and (22) and perform the limit $\lambda \to 0$. Using

$$\lambda^2 u''(\tau) = -\frac{x^4}{4}A''(x) - \frac{1}{2}x^3A'(x) + \frac{\lambda^2}{4}(x^2A'' + xA'), \quad (44)$$

we obtain

$$-\frac{x^4}{4}A''(x) - \frac{1}{2}x^3A'(x) + A(x) = -\frac{m}{2}x^2e^{A(x)-B(x)}, \quad (45)$$

$$-\frac{x^4}{4}B''(x) - \frac{1}{2}x^3B'(x) = \frac{1}{2}x^2(e^{A(x)-B(x)} - 1). \quad (46)$$

These equations determine the formal power series

$$A(x) = \sum_{n\geq 1} a_n x^{2n}, \quad (47)$$

$$B(x) = \sum_{n\geq 1} b_n x^{2n}, \quad (48)$$

where $a_n \equiv a_{nn}$ and $b_n \equiv b_{nn}$.

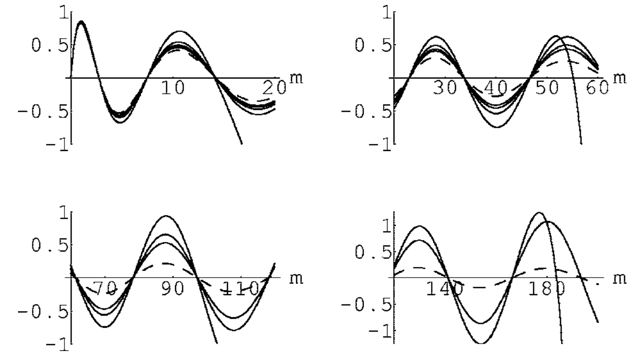

FIG. 4. Polynomials ϕ_n (solid lines) and limit ϕ (dashed lines) versus m. Upper left: $\phi_{10}, \phi_{20}, \phi_{30}, \phi_{40}, \phi_{50}, \phi$. Upper right: $\phi_{20}, \phi_{30}, \phi_{40}, \phi_{50}, \phi$. Lower left: $\phi_{30}, \phi_{40}, \phi_{50}, \phi$. Lower right: $\phi_{40}, \phi_{50}, \phi$. The maxima decrease and the minima increase with index n.

The equations become somewhat simpler in terms of $P(z)=A(z^{-1})$ and $Q(z)=B(z^{-1})$ and read

$$-\frac{1}{4}P''(z) + P(z) = -\frac{m}{2}z^{-2}e^{P(z)-Q(z)}, \quad (49)$$

$$-\frac{1}{4}Q''(z) = \frac{1}{2}z^{-2}(e^{P(z)-Q(z)} - 1). \quad (50)$$

$P(z)$ and $Q(z)$ must be expanded about the singular point $z = \infty$. [Formally this system is identical to the original system, Eqs. (2) and (3), via $x(t)=P(z)$, $y(t)=Q(z)+\ln(2z^2/m)$, $z = it/2$.]

From Eq. (41) we obtain $\phi_n(m)$. They are polynomials of order n in m:

$$\phi_n(m) = \sum_{k=1}^{n} \varphi_{nk}m^k. \quad (51)$$

The polynomials following $\phi_1(m)=2m$ are

$$\phi_2(m) = 2m - m^2, \quad (52)$$

$$\phi_3(m) = 2m - \frac{11}{9}m^2 + \frac{7}{36}m^3, \quad (53)$$

$$\phi_4(m) = 2m - \frac{119}{90}m^2 + \frac{49}{180}m^3 - \frac{37}{1800}m^4, \quad (54)$$

etc. The first term $2m$ is present in all polynomials. It is the golden rule result. Higher orders are easy to determine with a computer algebra system. Using a short but efficient Mathematica program the first 54 polynomials have been determined. The program is presented in the Appendix.

Figure 4 displays various polynomials $\phi_n(m)$ and the limit $\phi(m)$. ϕ is discussed below.

B. Convergence

There are strong numerical indications that ϕ_n converges to a limit function ϕ. The numerical data indicate a conver-

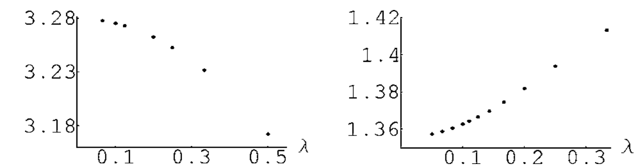

FIG. 5. Numerical data of $(\sinh \pi/\lambda)^2 E$ for $m=1$ (left) and $m=5$ (right) versus λ.

gence $\sim n^{-1}$; i.e., the data suggest an n dependence

$$\phi_n(m) = \phi(m) + \frac{\xi(m)}{n} + \frac{\theta(m)}{n^2} + \cdots . \qquad (55)$$

Due to the large number of high-quality data (54 polynomials with rational coefficients), the function $\phi(m)$ can be determined with high accuracy if m is not too large. For fixed m the numbers $x_n \equiv \{\phi_n(m)\}$ were analyzed as follows: The set $x_k, \ldots, x_n, \ldots, x_{54}$ was fitted to a function $a_k^{(1)} + b_k^{(1)}/n$. For k increasing towards 54, the $a_k^{(1)}$ and $b_k^{(1)}$ settle into a monotonic sequence. The "limits" $a_\infty^{(1)}$ and $b_\infty^{(1)}$ were determined by Wynn's ϵ algorithm with different degrees. Then the same procedure was repeated with the ansatz $a_k^{(2)} + b_k^{(2)}/n + c_k^{(2)}/n^2$, etc. The $a_\infty^{(k)}$ rapidly settle down to a constant with high precision. This was taken as $\phi(m)$.

The first four extrema of the limiting $\phi(m)$ are located at $m=0.977\,28$, 4.727 76, 10.4625, 18.211 with values 0.815 511, −0.532 665, 0.415 573, −0.34978.

The zeros of ϕ_n converge much more rapidly (even faster than exponentially). For example, the first zero of ϕ_{10} coincides with the limiting zero already in the first ten digits. The first six zeros of $\phi(m)$ are 2.761, 7.486, 14.218, 22.972, 33.757, 46.575.

A comparison with direct numerical solutions of Eqs. (2) and (3) has also been done. Figure 5 shows data for $(\sinh \pi/\lambda)^2 E$ for $m=1$ and $m=5$ and certain values of λ. These data were obtained using Mathematica. For $1/10 < \lambda < 1/2$ precision 24 was sufficient, but for the smallest λ the precision had to be increased up to 52 ($\lambda = 1/20$).

These data indicate, for $m=1$,

$$\left(\sinh \frac{\pi}{\lambda}\right)^2 E = 3.2796 - \text{const} \times \lambda^2 \qquad (56)$$

for small λ. The extrapolated value coincides very well with

$$\frac{1}{2}[\pi\phi(1)]^2 = 3.27959. \qquad (57)$$

For $m=5$ the extrapolated value is 1.355 which again compares very well with

$$\frac{1}{2}[\pi\phi(5)]^2 = 1.3555. \qquad (58)$$

For larger m the two methods still coincide very well albeit with somewhat lower precision. For example, for $m=20$ and $m=50$ the extrapolated values are 0.398 and 0.158, respectively, compared with 0.3982 and 0.1574 from ϕ.

V. FUNCTION $\phi(m)$

A. Expanding ϕ in powers of m

Expanding the solutions of Eqs. (49) and (50) in m we may obtain the first few coefficients of $\phi(m)$. To this end we insert the expansion

$$P(z) = \sum_{k=1}^{\infty} m^k P_k(z), \qquad (59)$$

$$Q(z) = \sum_{k=1}^{\infty} m^k Q_k(z) \qquad (60)$$

into Eqs. (49) and (50) and obtain

$$-\frac{1}{4}P_1'' + P_1 = -\frac{1}{2}z^{-2}, \qquad (61)$$

$$-\frac{1}{4}z^2 Q_1'' + \frac{1}{2}Q_1 = \frac{1}{2}P_1, \qquad (62)$$

$$-\frac{1}{4}z^2 Q_2'' + \frac{1}{2}Q_2 = \frac{1}{2}\left(P_2 + \frac{1}{2}(P_1 - Q_1)^2\right), \qquad (63)$$

etc., as well as

$$-\frac{1}{4}P_n'' + P_n = \frac{1}{4}Q_{n-1}'', \quad n \geqslant 2. \qquad (64)$$

As discussed previously, a_n and b_n are polynomials of order n in m which we write as

$$a_n = \sum_{k=1}^{n} p_{nk} m^k, \qquad (65)$$

$$b_n = \sum_{k=1}^{n} q_{nk} m^k. \qquad (66)$$

Therefore,

$$P_k(z) = \sum_{n \geqslant k} p_{nk} z^{-2n}, \qquad (67)$$

$$Q_k(z) = \sum_{n \geqslant k} q_{nk} z^{-2n}. \qquad (68)$$

p_{n1} is given by

$$p_{n1} = -2^{-2n+1}(2n-1)!. \qquad (69)$$

Since

$$\phi_n(m) = -\frac{2^{2n}}{(2n-1)!}a_n = -\sum_{k=1}^{n} \frac{2^{2n}}{(2n-1)!} p_{nk} m^k, \qquad (70)$$

this leads to the first term $2m$ in all ϕ_n which is the golden rule result. The other p_{nk} are related to q_{nk} by [compare Eq. (33)]

$$\frac{2^{2n}}{(2n-1)!}p_{nk} = \sum_{l=1}^{n-1} \frac{2^{2l}}{(2l-1)!}q_{l,k-1}, \quad k > 1. \tag{71}$$

The Q_k satisfy equations of the form

$$-\frac{1}{4}z^2 Q_k'' + \frac{1}{2}Q_k = \sum \sigma_{nk} z^{-2n}, \tag{72}$$

where the σ_{nk} are polynomials in the q_{nl} with $l<k$. This implies

$$q_{nk} = -\frac{2}{(2n-1)(n+1)}\sigma_{nk}. \tag{73}$$

In particular, since $\sigma_{n1}=p_{n1}/2$,

$$q_{n1} = 2^{-2n+1}\frac{(2n-2)!}{n+1}, \tag{74}$$

and therefore

$$\varphi_{n2} = -\frac{2^{2n}}{(2n-1)!}p_{n2} = -2\sum_{k=1}^{n-1}\frac{1}{(k+1)(2k-1)}. \tag{75}$$

This is the coefficient of m^2 of ϕ_n.

It is easy to determine the limit $n\to\infty$:

$$\lim_{n\to\infty}\varphi_{n2} = -\frac{2}{3}(1+\ln 4). \tag{76}$$

This is the exact coefficient of m^2 in ϕ.

To determine the next coefficient we need σ_{n2}. From Eq. (63) we find

$$\sigma_{n2} = \frac{1}{2}p_{n2} + \frac{1}{4}\sum_{r+s=n} c_r c_s, \tag{77}$$

with

$$c_n = p_{n1} - q_{n1} = -2^{-2n}\frac{(2n+1)!}{(n+1)(2n-1)}. \tag{78}$$

There seems no simple way to express this coefficient in terms of known functions. The numerical calculation poses no problems, and we obtain

$$\phi(m) = 2m - \frac{2}{3}(1+\ln 4)m^2 + 0.4746610m^3 + \cdots . \tag{79}$$

B. Analytic structure of $\phi(m)$

In this section I discuss some conjectures on the analytic structure of the limit function $\phi(m)$.

Consider first the high-order coefficients φ_{nk} in Eq. (51).

Figure 6 shows the values of $(k!)^2 2^{-k} k^{-1}|\varphi_{nk}|$ for the first 20 coefficients of $\phi_{24},\phi_{34},\phi_{44},\phi_{54}$. These data are not sufficient to indicate convergence, but they do suggest that $(k!)^2 2^{-k}|\varphi_{nk}|$ does not diverge faster that algebraically. In any case they indicate

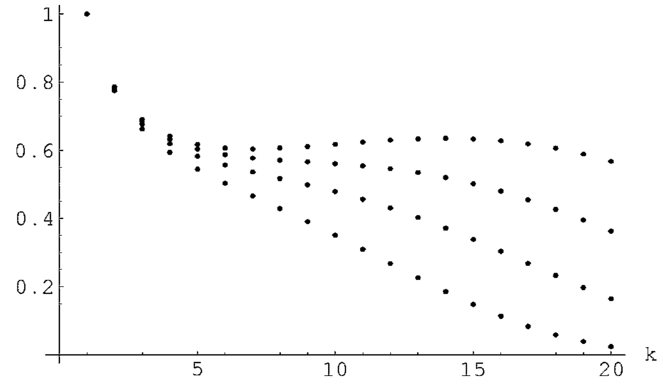

FIG. 6. Values of $(k!)^2 2^{-k} k^{-1}|\varphi_{nk}|$ versus k for n=24, 34, 44, 54. The lowest points correspond to ϕ_{24} and the highest to ϕ_{54}.

$$|\varphi_{nk}| < \frac{c^k}{(k!)^2} \tag{80}$$

for some constant c.

This inequality also follows from the much stronger inequality

$$(k+1)^2\varphi_{n,k-1}\varphi_{n,k+1} < k^2\varphi_{nk}^2, \tag{81}$$

which is found to be true for *all* coefficients of the 54 polynomials. This suggests that the limit function satisfies the same inequalities.

We conclude that ϕ is analytic in the whole complex plane, satisfies Eq. (80) and therefore is an entire function of m.

We saw previously that ϕ has (probably infinitely many) real and simple roots. What about complex roots?

Figure 7 shows the roots of $\phi_{24},\phi_{34},\phi_{44},\phi_{54}$ that are located in the upper half plane. The innermost points refer to ϕ_{24} and the outermost ones to ϕ_{54}. Apparently the complex roots move more and more to infinity with increasing n. This indicates that the limit function $\phi(m)$ has only real and nonnegative roots.

Denote the positive roots by m_n. Figure 8 shows $\sqrt{m_n}$ versus n. The plot is almost linear with a slope very close to 1. Careful analysis similar to Sec. IV B indicates that the slope

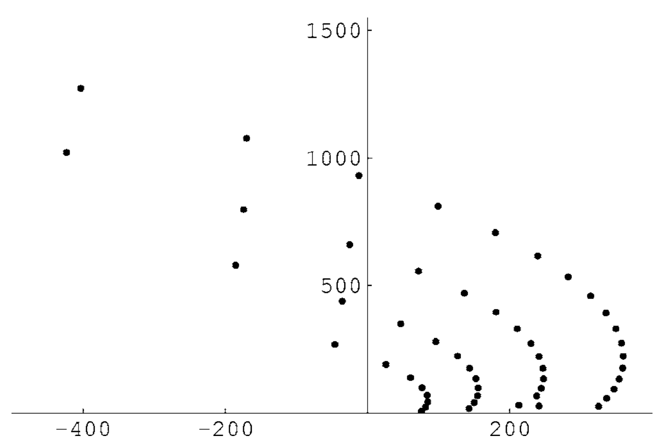

FIG. 7. Complex roots in the upper half plane of $\phi_{24},\phi_{34},\phi_{44},\phi_{54}$.

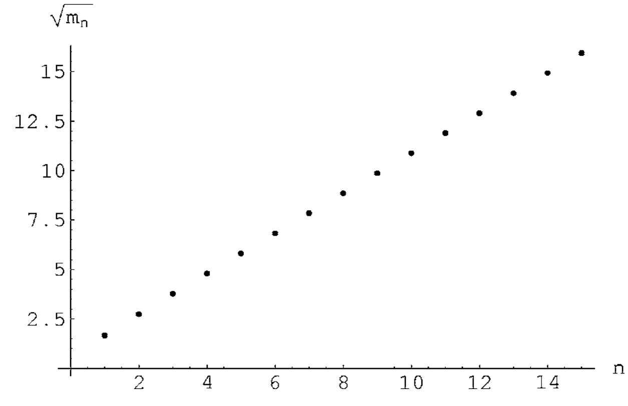

FIG. 8. Square root of zeros m_n of $\phi(m)$ versus n.

is slightly larger than 1. Using the 15 known roots suggests that asymptotically, for large n,

$$\sqrt{m_n} \sim 1.0106n + 0.770. \tag{82}$$

In particular, the series Σm_n^{-1} converges. Therefore, according to Hadamard's factorization theorem [18], ϕ may be written in the form

$$\phi(z) = e^{g(z)} 2z \prod_{n=1}^{\infty} \left(1 - \frac{z}{m_n}\right), \tag{83}$$

with an entire function $g(z)$. (In the following I write m for real and z for complex arguments.)

There are strong indications that $g(z) \equiv 0$. Indeed, if inequality (80) is satisfied, $\phi(z)$ is an entire function of order $\leqslant 1/2$ which implies that $g(z)$ is a constant (see, for example Ref. [18]).

An entire function $f(z)$ has order ρ and type τ if [18]

$$\overline{\lim}_{r\to\infty} r^{-\rho} \ln M(r) = \tau, \tag{84}$$

where $M(r)$ is the maximum modulus $M(r) = \sup|f(z)|$ on $|z| = r$.

We can use this relation to estimate the order directly. Since the coefficients of the ϕ_n alternate in sign, at fixed $|z|$, $|\phi_n(z)|$ and $|\phi(z)|$ take their maxima on the negative real axis.

Figure 9 shows data for $|\phi(-m)|$ (extrapolated from the ϕ_n as discussed in Sec. IV B) versus m. The lower points correspond to $m^{-1/2} \ln|\phi(-m)|$ and the upper ones to $m^{-1/2} \ln|\sqrt{-m}\phi(-m)|$. The lower points seem to increase slowly with m, and the upper ones seem to be constant or decrease very slowly. In any case, these data are consistent with order 1/2. They suggest

$$\phi(-m) \sim (-m)^{-\alpha} \exp\{-\tau\sqrt{-m}\}, \tag{85}$$

with $\alpha \lesssim 0.5$ and type $\tau \sim 3$.

The preceding deliberations indicate that $\phi(z)$ can be written as an infinite product

$$\phi(z) = 2z \prod_{n=1}^{\infty} \left(1 - \frac{z}{m_n}\right). \tag{86}$$

Such a product has an order equal to the convergence exponent of its zeros [18]. In our case this is 1/2 [see Eq. (82)].

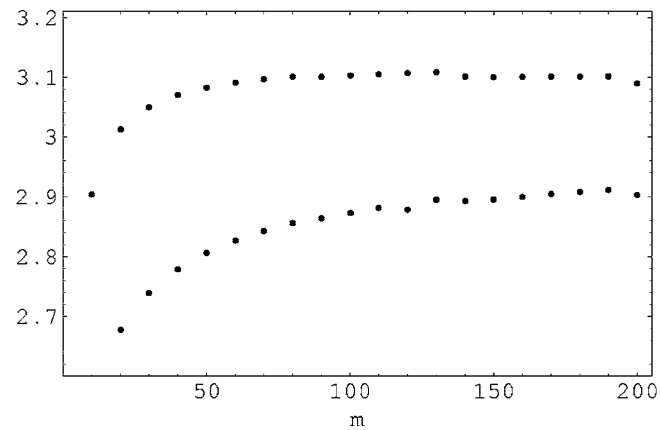

FIG. 9. $m^{-1/2} \ln|\phi(-m)|$ (lower points) and $m^{-1/2} \ln|\sqrt{-m}\phi(-m)|$ (upper points) versus m.

The type of this product is $\tau = \pi/\kappa$ where $\kappa = \lim_{n\to\infty} n^{-1}\sqrt{m_n}$. With $\kappa = 1.0106$ we obtain $\tau = 3.109$ which is consistent with Fig. 9.

Perhaps the best known example of such a product is the infinite product for $\sin z$. In the form

$$\sqrt{z} \sin \pi\sqrt{z} = \pi z \prod_{n=1}^{\infty} \left(1 - \frac{z}{n^2}\right), \tag{87}$$

it looks strikingly similar to Eq. (86). Moreover, in both cases the roots are quadratic in n. Both functions have order 1/2 and the types are almost identical (π/κ versus π). There are, of course, differences for large z.

For further discussion let us define a "numerical" ϕ_{num} by Eq. (86) where the numerical values for the known first 15 roots are used together with the asymptotic estimate, Eq. (82) for the higher roots. For positive m this ϕ_{num} coincides very well with the extrapolated values of ϕ (typically the error is $< 10^{-4}$). The coefficient of m^2 in ϕ_{num} differs from the exact value Eq. (76) by an error of 3×10^{-6}.

Figure 10 shows ratios $\phi_n(m)/\phi_{num}(m)$ for various n and m. Figure 10(a) show this ratio on the negative real axis for $-20 < m < 0$ and various n. The ratios seem to converge to 1 for $n \to \infty$. In order to check this, Fig. 10(b) shows the ratios for $m = -20$ (upper curve) and $m = -50$ (lower curve) for all n versus n^{-1}. It looks as if the number of polynomials is insufficient for definite conclusions. However, if analyzed as in Sec. IV B, the extrapolated value is an impressive 1.000 for both $m = -20$ and $m = -50$. The reason probably is that the

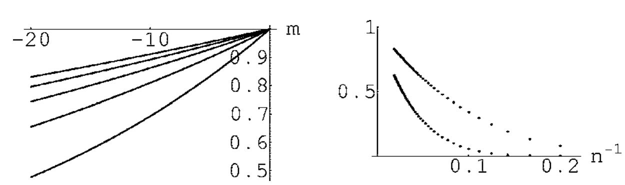

FIG. 10. Ratios $\phi_n(m)/\phi_{num}(m)$ on the negative real axis. Left: ratio versus m for $n = 14, 24, 34, 44, 54$ (from bottom to top). Right: ratios for $m = -20$ (upper curve) and $m = -50$ (lower curve) versus n^{-1}.

data are very precise and that Eq. (55) really describes the n dependence.

The situation is very similar on the imaginary axis. ϕ_{num} seems to be a very good approximation to the true ϕ on the whole complex plane.

VI. MINIMAL SOLUTION

The oscillator energy in the high-frequency limit seems to have a very simple structure. In fact the structure seems to be the simplest possible compatible with the three known constraints.

(i) The final oscillator energy E must be non-negative.

(ii) The golden rule limit $m \to 0$ must be satisfied.

(iii) There must be an infinite number of m_i, which leaves the oscillator at rest.

The "minimal solution" which satisfies just these constraints would have the form

$$E = 2\pi^2 \phi(m)^2 \exp\{-2\pi/\lambda\}, \tag{88}$$

where π/λ is the decay constant from the golden rule and $\phi(m)$ has an infinite number of positive roots and behaves as $2m$ for small m. The simplest possible ϕ would have the product form, Eq. (86). Remarkably, as discussed above, there are strong indications that this is precisely the form of the solution in the high-frequency domain.

APPENDIX: MATHEMATICA PROGRAM FOR $\phi_n(m)$

The Mathematica program first calls the package Combinatorica.

≪DiscreteMath'Combinatorica'

Then a module "serex" is defined by

$$\text{serex}[m\_] := \text{Module}[\{ph, xh, yh\}, ph = \text{Partitions}[m];$$

$$xh = \text{Table}[\text{Map}[c, ph[[n]]], \{n, 1, \text{Length}[ph]\}];$$

$$yh = \text{Map}[\text{Apply}[\text{Times}, \#]\&, xh];$$

$$\text{Apply}[\text{Plus}, yh/\sum_{k=1}^{m} \text{Map}[\text{Count}[\#, k]\&, ph]!]]$$

the rule tc is initialized

$$\text{tc} = \left\{ a[1] \to -\frac{m}{2}, b[1] \to \frac{m}{4} \right\}$$

and the module plC is defined by

$$\text{plC}[n\_] := \text{Module}[\{h1, h2, \text{sl}\},$$

$$h1 = \text{Expand}\left[-\frac{n}{2}(2n+1)b[n] - \frac{1}{2}(\text{serex}[n] /. \, c[k\_] \to a[k] - b[k]) /. \, \text{tc} \right];$$

$$h2 = \text{Expand}\left[a[n] - \frac{n-1}{2}(2n-1)a[n-1] + \frac{m}{2}(\text{serex}[n-1] /. \, c[k\_] \to a[k] - b[k]) /. \, \text{tc} \right];$$

$$\text{sl} = \text{Solve}[\{h1 == 0, h2 == 0\}, \{a[n], b[n]\}];$$

$$\text{tc} = \text{Flatten}[\text{Join}[\text{tc}, \text{sl}]]$$

Rule tc is built up by successively calling plC, starting from $n=2$ as in

$$\text{Table}[\text{plC}[n], \{n, 2, 54\}]$$

54 was the maximum number feasible on my PC. The polynomial ϕ_n of order n is given by

$$\text{Expand}\left[-2^{2n} \frac{a[n]}{(2n-1)!} /. \, \text{tc} \right]$$

[1] D. Rapp and T. Kassal, Chem. Rev. (Washington, D.C.) **69**, 61 (1969).
[2] J. Chesnoy and G. M. Gale, Adv. Chem. Phys. **70**, 297 (1988).
[3] C. B. Harris, D. E. Smith, and D. J. Russell, Chem. Rev. (Washington, D.C.) **90**, 481 (1990).
[4] J. C. Owrutsky, D. Raftery, and R. M. Hochstrasser, Annu. Rev. Phys. Chem. **45**, 519 (1994).
[5] D. Rapp, J. Chem. Phys. **32**, 735 (1960).
[6] J. D. Kelley and M. Wolfsberg, J. Chem. Phys. **44**, 324 (1966).
[7] D. Secrest, J. Chem. Phys. **51**, 421 (1969).
[8] L. Gottdiener and R. Carmona, J. Chem. Phys. **70**, 4207 (1979).
[9] G. Benettin, A. Carati, and P. Sempio, J. Stat. Phys. **73**, 175 (1993).
[10] E. B. Alterman and D. J. Wilson, J. Chem. Phys. **42**, 1957 (1965).
[11] A. Carati, L. Galgani, and B. Pozzi, Phys. Rev. Lett. **90**, 010601 (2003).
[12] D. Secrest and B. R. Johnson, J. Chem. Phys. **45**, 4556 (1966).
[13] M. Teubner, Phys. Rev. E **65**, 031204 (2002).
[14] M. Teubner, Phys. Rev. E **70**, 061104 (2004).
[15] I. S. Gradshteyn and I. M. Ryzhik, *Table of Integrals, Series, and Products* (Academic Press, New York, 1980).
[16] A. Carati, G. Benettin, and L. Galgani, Commun. Math. Phys. **150**, 321 (1992).
[17] G. Benettin, P. Hjorth, and S. Sempio, J. Stat. Phys. **94**, 871 (1999).
[18] R. P. Boas, *Entire Functions* (Academic Press, New York, 1954).